Literature review

Precipitation in creep resistant austenitic stainless steels

T. Sourmail

Austenitic stainless steels have for some time been used as superheater tubes in the electricity generation industries in harsh environments with temperatures as high as 650°C at pressures of some 200 atm; they are expected to provide reliable service for 30 years or more. Their detailed mechanical properties are dependent on the stability of the microstructure, particularly the formation, dissolution, and coarsening of precipitates. Although the precipitation processes have been studied extensively, there remain important discrepancies. It is known that small changes in the chemical composition or thermomechanical processing can profoundly influence the evolution of the microstructure. This review focuses on precipitation in creep resistant austenitic stainless steels, in particular wrought heat resistant grades containing niobium and titanium additions. Conventional alloys such as 18–8 and 16–10 are included together with the new NF709 (20–25) and other recent variants. Precipitates forming in age hardening austenitic stainless steels are only briefly presented. Many studies have shown that MX is not a stoichiometric phase, and that chromium can be incorporated in the metal sublattice. Furthermore, the reported compositions show considerable variation. These studies are assessed and an explanation is offered, in terms of the Gibbs–Thompson effect, for the variation. A rational consideration of all the results suggests a size dependence in line with capillarity considerations. The MX phase does not form in isolation; its stability also depends on the formation of $M_{23}C_6$. The literature reveals that NbC is more stable than $M_{23}C_6$ but the case for TiC is less certain. The formation of Z phase in nitrogen bearing steels is a further complicating factor, and it is concluded that its formation is not adequately understood. This is unlike the case for $M_{23}C_6$, where there is consistent reporting in the literature. Finally, work on the M_6C carbide in austenitic stainless steels is critically assessed. It is found that its detailed composition is not well characterised and that there are no general rules apparent about its formation. The review also covers intermetallic compounds such as σ phase. It is clear that chromium concentrations in excess of 18 wt-%, combined with a low carbon concentration, promote the formation of σ phase. This has implications particularly for steels containing niobium and titanium, both of which getter carbon. Other compounds reviewed include χ and G phases, which form at high temperatures and during very long aging such as that encountered in service. **MST/4721**

The author is in the Department of Materials Science and Metallurgy, University of Cambridge, Pembroke Street, Cambridge CB2 3QZ, UK.

Introduction

Austenitic stainless steels are, by far, the most widely used stainless steels, constituting 70–80% of stainless production.[1] With excellent corrosion resistance and mechanical properties at high temperatures, they are choice materials for powerplant tubes which have to operate at temperatures above 950 K, or for aeroengines. The important role of precipitation in the achievement of good creep properties has been understood for a long time and extensively studied. Although some phases are now well documented, there are still contradictions and missing thermodynamic data; in particular, there is only a limited amount of information about phases such as Z phase or Cr_3Ni_2SiN, which can be predominant precipitates in nitrogen bearing steels. The present paper is a review of common precipitates in austenitic stainless steels, in particular wrought heat resistant steels of the AISI 300 family and 20–25 steels. Precipitates forming in age hardening austenitic stainless steels are only briefly presented, having been previously reviewed by other authors.

COMPOSITION AND CONSTITUENTS

Austenitic stainless steels are essentially alloys of Fe–Cr–Ni, which owe their name to their room temperature austenitic structure. The addition of chromium has long been known to improve corrosion resistance. Chromium is also a ‘ferrite stabiliser’, and Fe–Cr stainless steels have a ferritic structure, or possibly martensitic depending on the heat treatment. The addition of austenite stabilising elements in sufficient quantities can allow an austenitic structure to be stable at all temperatures.

Nickel is the basic substitutional element used for austenite stabilisation. The equilibrium phases depend on the proportion of the three elements, which is well illustrated in an isothermal section of the ternary diagram for Fe–Cr–Ni (Fig. 1) calculated using MTDATA.[2]

Often, alloying elements, either interstitial such as carbon or nitrogen, or substitutional such as Mo, Mn, Ti, Nb, V, W, Cu, Al, etc. are used to obtain the required properties.

This review was a runner-up in the inaugural *MST* Literature Review Prize competition, set up to encourage the preparation of critical literature reviews by students as an essential part of study for a higher degree in the materials field, and subsequently to make the best of these available to a wider readership.

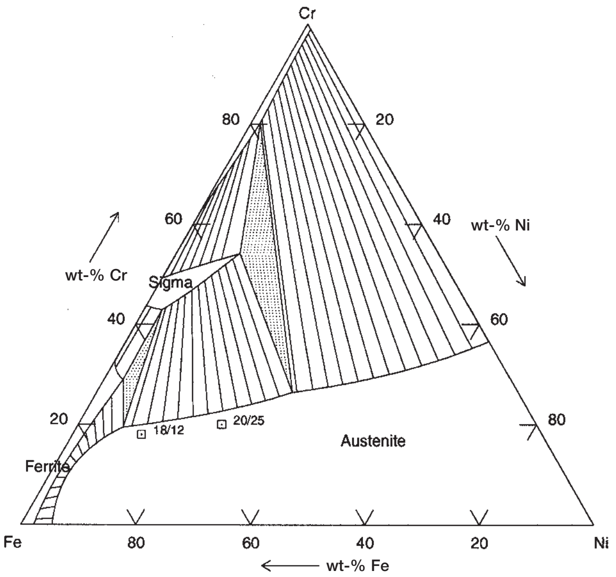

1 Isothermal section of Fe–Cr–Ni diagram at 750°C: typical 18Cr–12Ni (wt-%) steel lies in austenitic field, calculated using MTDATA and SGTE database

They can be classified as ferrite stabilisers or austenite stabilisers, and their effect in this respect is often approximated using the notion of chromium and nickel equivalents, calculated by formulae such as[3]

$$\mathrm{Ni_{eq}} = [\mathrm{Ni}] + [\mathrm{Co}] + 0\cdot5[\mathrm{Mn}] + 30[\mathrm{C}] + 0\cdot3[\mathrm{Cu}] + 25[\mathrm{N}] \quad (\text{wt-\%})$$

$$\mathrm{Cr_{eq}} = [\mathrm{Cr}] + 2\cdot0[\mathrm{Si}] + 1\cdot5[\mathrm{Mo}] + 5\cdot5[\mathrm{Al}] + 1\cdot75[\mathrm{Nb}] + 1\cdot5[\mathrm{Ti}] + 0\cdot75[\mathrm{W}] \quad (\text{wt-\%})$$

In the above example, the composition is given in wt-%. The use of such formulae is not always straightforward, as they refer to the austenite content, which is modified by various precipitation reactions involving these elements.

Whether the austenitic structure is retained at room temperature depends on the martensite start temperature M_s. Several empirical formulae have been derived to describe the effect of chemical composition on M_s, for example[1]

$$M_s(^\circ\mathrm{C}) = 502 - 810[\mathrm{C}] - 1230[\mathrm{N}] - 13[\mathrm{Mn}] - 30[\mathrm{Ni}] - 12[\mathrm{Cr}] - 54[\mathrm{Cu}] - 6[\mathrm{Mo}] \quad (\text{wt-\%})$$

A typical type 304 austenitic stainless steel has an M_s that is well below room temperature. However, it should be kept in mind that deformation induced martensite formation can occur well above M_s. The temperature M_{d30} is that at which 50% of the structure has transformed to martensite at a true strain of 30%. Again, formulae such as

$$M_{d30}(^\circ\mathrm{C}) = 497 - 462[\mathrm{C+N}] - 9\cdot2[\mathrm{Si}] - 8\cdot1[\mathrm{Mn}] - 20[\mathrm{Ni}] - 13\cdot7[\mathrm{Cr}] - 18\cdot5[\mathrm{Mo}] \quad (\text{wt-\%})$$

have been derived to describe the effect of alloying elements.[1]

At high temperatures, a steel containing 18 wt-%Cr, 12 wt-%Ni should be fully austenitic. However, the addition of alloying elements often results in the formation of carbides, nitrides, and intermetallics. These phases are not always desirable, and a good knowledge of precipitation reactions is required to avoid deterioration of mechanical or chemical properties. A good example is the sensitisation of non-stabilised austenitic stainless steels: sensitisation occurs when the precipitate $M_{23}C_6$ forms at grain boundaries, depleting the chromium content in the vicinity, which eventually results in intergranular corrosion. This can be avoided by tying up the carbon with strong carbide formers such as titanium. The steel is then termed ‘stabilised’. These second phases are presented in detail below.

GRADES OF AUSTENITIC STAINLESS STEEL

From a simple type 304 alloy to the recent NF709, austenitic stainless steel composition covers a wide range (Table 1).[4,5] The two main alloying elements are chromium and nickel, so the steels are often referred to by their contents of these elements. For example, 18–10 refers to an austenitic stainless steel with 18 wt-%Cr, 10 wt-%Ni.

The AISI 300 specifications for the compositions of various austenitic stainless steels (wt-%) are given in Table 2, along with those for other heat resistant austenitic stainless steels.[4]

Grades denoted L contain low carbon (0·03 wt-%) and those denoted N contain nitrogen (for example, 316LN). Most often used as creep resistant steels are types 316, 321, and 347, or alloys containing all of Mo, Nb, and Ti. There are many other variants of these compositions, such as the Japanese SUS300 series which mirrors the AISI 300 series, but with sometimes the addition of both titanium and niobium. For convenience, as sometimes found in the literature, the AISI 300 designation is used in the present paper even for steels not strictly belonging to it, for example a 316 with titanium addition.

In the present review, it is not the intention to describe the precipitation sequences in all the various grades of creep resistant austenitic stainless steels, but rather to examine the occurrence of the various precipitates in such a way that the precipitation behaviour of non-documented grades can be inferred from the conclusions reached.

There is a large amount of information on precipitation phenomena in the 300 series of alloys, which have been used widely as creep resistant steels. The same is true for 20Cr–25Ni steels. However, it appears that the long term behaviour of (Ti+Al) alloyed austenitic stainless steels (type A286) is very little documented.[6] This is possibly because production difficulties have restricted the application of such steels to parts requiring relatively small ingot sizes (aeroengine turbine discs), the design life of which is much shorter than the few 100 000 h required for a steam plant.[7]

ROLE OF ALLOYING ELEMENTS

Manganese has been introduced in austenitic stainless steels as a substitute for nickel during shortages in the international market, or for economic reasons. The nickel content can be halved to 4 wt-% by the addition of 2–6 wt-%Mn. However, although the austenitic structure is achieved, such steels do not exhibit the same corrosion resistance as an 18–8 steel. Manganese is also used to increase the solubility of nitrogen in austenite.

Molybdenum is, on the other hand, a ferrite stabiliser. It improves the creep properties of stainless steels by solid solution hardening. It also facilitates carbide precipitation.

Table 1 Compositions of two austenitic stainless steels, wt-%

	C	Si	Mn	P	Cr	Mo	Ni	B	N	Nb	Ti	Fe
Type 304 (Ref. 4)	⩽0·07	~0	⩽2·00	0·04	17–19	~0	8–10	~0	~0	~0	~0	Bal.
NF709 (Ref. 5)	0·06	0·40	1·00	0·006	20	1·5	25	0·005	0·167	0·26	0·05	Bal.

Table 2 Compositions of AISI 300 series and other examples* of heat resistant austenitic stainless steels, wt-%

	C max.	Si max.	Mn max.	Cr	Mo	Ni	Al	Nb	Ti	V	Fe
301	0·15	1·00	2·00	16–18	...	6–8	...	...	...	...	Bal.
302	0·15	1·00	2·00	17–19	...	8–10	...	...	...	...	Bal.
304	0·08	1·00	2·00	18–20	...	8–12	...	...	...	...	Bal.
310	0·25	1·50	2·00	24–26	...	19–22	...	...	...	...	Bal.
316	0·08	1·00	2·00	16–18	2·0–3·0	10–14	...	...	...	...	Bal.
321	0·08	1·00	2·00	17–19	...	9–12	...	...	5 × %C min.	...	Bal.
347	0·08	1·00	2·00	17–19	...	9–13	...	10 × %C min.	...	...	Bal.
E1250*	0·1	0·5	6·0	15·0	...	10·0	...	...	...	0·25	Bal.
20–25 Nb	0·05	1·0	1·0	20·0	...	25·0	...	0·7	...	...	Bal.
A286	0·05	1·0	1·0	15·0	1·2	26·0	~0·18	...	~1·9	~0·25	Bal.

*E1250 is Esshete 1250.

However, it promotes σ and Laves phase formation on long term aging.

Stabilising elements such as Nb, Ti, and V greatly improve the creep strength of austenitic stainless steels, mainly by precipitating fine carbides intragranularly. However, they reduce the creep ductility. The ratio to carbon in which they are added is important to maximise the strengthening effect and avoid precipitation of detrimental phases. They can also have a solid solution strengthening effect.

Carbon acts principally by solid solution strengthening in non-stabilised grades, but mainly by precipitation strengthening when Nb, T, or V is present.

Nitrogen is a strong austenite stabiliser. It also has a role in increasing the creep life of austenitic stainless steels: it can act like carbon in stabilised stainless steel by precipitating in the form of titanium or niobium nitrides, but the nitrogen remaining in solid solution has a much greater strengthening effect than that of carbon. It has been believed also to lower the diffusivity of chromium and carbon in the matrix, therefore delaying coalescence of precipitates.[1,4] However, more recent results indicate that nitrogen enhances chromium diffusion, but retards the nucleation of $M_{23}C_6$ because of its low solubility in this carbide.[8]

Carbides and nitrides

MX PRECIPITATES

The formation of MX precipitates in austenitic stainless steels occurs when strong carbide/nitride formers (Ti, Nb, V, Zr, Ta, etc.) are added to the alloy. These additions have the following two purposes.

1. Stabilising the alloy against intergranular corrosion: when stabilisation is the first aim, a stabilising heat treatment is conducted at 840–900°C for several hours before service. Most of the carbon is then 'tied up' by precipitation of MC.
2. Providing good creep resistance: when this is the first aim, a solution heat treatment is given to dissolve as much MX as possible. Subsequent precipitation occurs during creep and increases strength. A typical solution treatment is 30–60 min at temperatures between 1100 and 1250°C.

The second use is focused on below.

Many studies have concentrated on MX precipitation, but also on the appropriate content necessary to obtain optimum properties. The solubility of the MX precipitates and the stoichiometry are essential in determining the behaviour of the steel with regard to precipitation.

Table 3 Lattice parameters of some MX precipitates

MX	*a*, nm	Ref.
NbN	0·439	JCPDS 38–1155
NbC	0·447	JCPDS 38–1364
TiN	0·424	JCPDS 38–1420
TiC	0·433	JCPDS 32–1383

Structure and features of precipitation

The MX carbonitrides have a NaCl face centred cubic (fcc) structure, with lattice parameters as given in Table 3. Often, measured lattice parameters have intermediate values, reflecting the existence of a solid solution between the different carbonitrides.

The MX precipitates usually form on dislocations within the matrix, on stacking faults (most often with TiC), and on twin and grain boundaries. They have a characteristic cuboidal shape after sufficient aging.

Solubility of MX carbides in austenite

Stabilisers such as titanium or niobium have long been known to reduce the solubility of carbon in austenite. Early studies of the problem comprised the determination of two parameters: H, the enthalpy of solution, and A, a constant as in

$$\log[\mathrm{M}][\mathrm{X}] = A - \frac{H}{T}$$

where [M] is the concentration in wt-% of the stabilising element in solution in the matrix (similarly for [X]) and T is the temperature in K. The product [M][X] is often referred to as the solubility product. Strictly speaking, H is expressed in K^{-1}.

The two following relationships can be found in many publications (for example, Refs. 3 and 4)

$$\log[\mathrm{Ti}][\mathrm{C}] = 2{\cdot}97 - \frac{6780}{T}$$

$$\log[\mathrm{Nb}][\mathrm{C}] = 4{\cdot}55 - \frac{9350}{T}$$

They are essentially valid for a typical 18–12 steel. For a 20–25 steel, Kikuchi *et al.*[9] used, for TiC, $H = 10\ 475\ \mathrm{K}^{-1}$, $A = 3{\cdot}42$ and, for NbC, $H = 7900\ \mathrm{K}^{-1}$ and $A = 4{\cdot}92$, but it is not clear whether these values have been measured for 20–25. As shown in their work, the solubility is an important factor in the achievement of good creep properties. They demonstrated that adding M and X in excess of their solubility limits resulted in coarse MX in the matrix and induced faster coarsening of MX later precipitated.[9] However, until this limit is reached, the more M and X that are added the better, because more MX particles will be formed.

It is therefore clear that knowing the solubility limits of MX carbides is important. However, modern high temperature austenitic stainless steels often contain both carbon and nitrogen, and more than one strong carbide former ((Ti + Nb), (Nb + V), etc.), and relationships as above are of limited use when it comes to estimating the solubility of multicomponent carbonitrides (for example, (Ti,Nb)(C,N)).

Recently, some studies have proposed different approaches to the problem of the solubility of multicomponent carbonitrides in austenite.[10–12] For example, Rios[10] proposed for Nb(C,N)

$$(\%\mathrm{Nb})[(\%\mathrm{C})/K_{\mathrm{C}}^{1\cdot5}+(\%\mathrm{N})/K_{\mathrm{N}}^{1\cdot15}]^{0\cdot87}=1$$

where

$$\log\ K_{\mathrm{C}}=\Delta G^{\circ}_{\mathrm{NbC}_{0\cdot87}}/RT$$

$$\log\ K_{\mathrm{N}}=\Delta G^{\circ}_{\mathrm{NbN}_{0\cdot87}}/RT$$

and K is the equilibrium constant, ΔG° is the standard free energy change, and R is the universal gas constant.

However, it must be noted that all these studies deal with MX in austenite for microalloyed steels. It seems clear, from the literature, that the presence of nickel and chromium introduces a further difficulty in austenitic stainless steels, i.e. the formation of Z phase.

There is general agreement that Z phase (CrNbN) forms in niobium stabilised austenitic stainless steels, with a sufficient amount of nitrogen. In fact, it seems that as soon as 0·06 wt-%N is present in a typical 347 steel, Z phase can be expected.[13]

Moreover, in Cr–Ni steels, MX precipitates have been reported to start growing largely understoichiometric.[14,15] No approaches have been found in the literature dealing with the solubility of multicomponent carbonitrides in austenitic stainless steels susceptible to Z phase formation. Indeed, Z phase is even absent from the Scientific Group Thermodata Europe (SGTE) thermodynamic databases accessed by programs such as MTDATA or Thermo-Calc.

Formation and stoichiometry of MX precipitates

A number of studies have been devoted to determination of the correct quantities of M and X to use in order to achieve optimum mechanical properties. As stated above, one factor is the solubility of MX. This has been clearly outlined by the work of Kikuchi *et al.*[9]

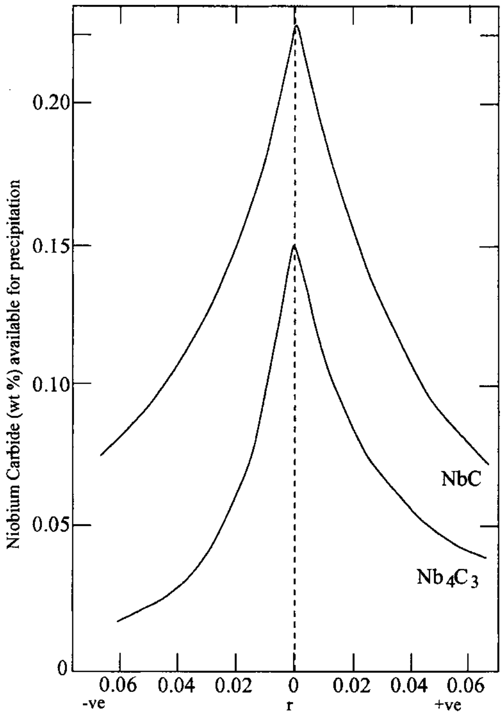

2 Amount of niobium carbide available for precipitation of 923 K (after solution treatment at 1373 K) as function of degree of deviation from stoichiometry r, defined by $r=pB_{\mathrm{T}}-qA_{\mathrm{T}}$, where p and q are mass fractions of A and B in compound AB_n, and A_{T} and B_{T} are mass fractions of these elements in alloy[16]

The second factor is the proportion of each element that has to be added, in such a way as to maximise the amount of precipitation for a given product [M][X]. It is also important to know, if stoichiometry is not respected, which of the elements is in excess, as this may influence the precipitation sequence.

Wadsworth *et al.*[16] proposed a quantitative approach to stoichiometry, and showed that the amount of precipitate that can form falls quite sharply when M and X are not added in proportions corresponding to the composition of the expected carbide (Fig. 2). Using the data of Keown and Pickering,[17] they showed that optimum creep lives were obtained when the Nb/C ratio matched the stoichiometry Nb_4C_3 (for 18–12 or 18–10 steels).

Other studies[9,18] showed that optimum creep life was obtained for a Nb/C atomic ratio of 1 : 1 for 20–25 steel). The work done by Kikuchi *et al.*[9] does not highlight any serious contradiction, since the first composition they tried around the atomic ratio 1 : 1 was 2 : 1, which means that any variation within this interval was not investigated. However, Adamson and Martin[18] give results for the weight ratios 8 : 1 and 10 : 1 (respectively, atomic ratios 1 : 1 and 4 : 3), but find better creep properties for the 1 : 1 atomic ratio. A possible explanation is that NbC actually forms with the stoichiometry 1 : 1 in 20–25 steels. It seems important to note that all these studies rely on relatively short term creep tests (on average, less than 1000 h). No study has been found in the literature that confirms the importance of stoichiometric addition for long term creep properties. Moreover, this explanation of the good creep properties of steels with stoichiometric additions of M and X assumes that MX precipitates form with their final stoichiometry, which has been proved to be wrong by various authors.

The non-stoichiometry of MX precipitates in 18–12 austenitic stainless steels has been confirmed by microprobe analysis.[14,15] The authors noted that MX was largely substoichiometric for short aging (typically 3 h at 750°C), and contained a large amount of chromium substituting for M (Ti, Nb, V, etc.). They proposed the following explanations. As MX has a lattice parameter larger than that of the austenite, a flow of vacancies is needed for the growth of MX and stress is generated. The substitution of M by chromium and the low carbon content both reduce the lattice parameter. Moreover, chromium is readily available while M has to diffuse over long distances. The formation of substoichiometric, carbon depleted MX precipitates is therefore kinetically advantageous. In more theoretical terms, this corresponds to two effects. Capillarity is likely to modify substantially the local equilibrium as the precipitates are very small. In fact, the composition changes reported by these authors correlate with size changes. The second effect is the modification of local equilibrium to satisfy simultaneously the flux balance for different solutes. This effect could strongly influence the composition of MX, since the diffusivities of the elements involved are very different. It would similarly correlate with a size change unless the precipitates are only coarsening.

However, stoichiometric carbides still have a lower free energy and, during further aging, they grow at the expense of substoichiometric carbides. This is because, according to Adrén *et al.*, the diffusivity of metallic elements within MX precipitates is so small that these precipitates cannot change composition.[14]

Z PHASE

The Z phase is a complex carbonitride which forms in niobium stabilised austenitic stainless steels containing a relatively high level of nitrogen. It has only recently been discovered, with its structure being fully determined by Jack and Jack in 1972,[19] and it appears from the most recent reviews (for example, Ref. 3) that the conditions of its formation are not very clear, and even less clear is its relative stability when compared with other carbonitrides.

Structure and composition

The structure of Z phase is commonly accepted to be that described by Jack and Jack:[19] it has a tetragonal unit cell (space group *P4/nmm*), with $a = 0{\cdot}3037$ nm and $c = 0{\cdot}7391$ nm. The unit cell is obtained by the ordering of Cr, Nb, and N atoms, the formula being $Cr_2Nb_2N_2$ per unit cell. Vodárek[20] reports the following orientation relationship for Z phase in a type 316LN

$$(001)_Z \| (001)_\gamma$$

$$[1\bar{1}0]_Z \| [100]_\gamma$$

In contrast with MX precipitates, it seems that Z phase dissolves few (if any) substitutional elements. Raghavan *et al.*[21] suggest that it can dissolve carbon, and write CrNb(CN), without giving any evidence for this. The absence of a CrNbC phase suggests that if carbon can dissolve in Z phase, it can do so only within limits. Also, when niobium is in sufficient quantity, both Z phase and NbC are found.

Occurrence

The Z phase is seldom reported, even in alloys liable to form it on aging. This could be a result of its composition and its general features of formation, which are not very different from those of common MX precipitates.

It generally forms on grain boundaries, very rapidly, but also on twin boundaries and within the matrix, where it is associated with dislocations.[22] When it forms, it is usually as a fine dispersion of particles (*see* Refs. 13, 21, and 22), which makes it an interesting phase when good creep properties are sought. The morphology has been reported to be either cuboidal[22] or rodlike.[14]

There is good agreement that Z phase forms at high temperature: Raghavan *et al.*[21] report its formation during annealing (1 h at 1300 K) of an 18–12 steel containing 0·3 wt-%Nb and 0·09 wt-%N, with an orientation relationship indicating that these are not residual particles. After aging for 8000 h at 866 K, it is still the predominant precipitate. Few $M_{23}C_6$ and σ phase particles are present. These authors indicate that a 10 s heat treatment at 1573 K is sufficient to dissolve all the Z phase particles; this is not inconsistent with the work of Robinson and Jack[22] which locates the solvus of the Z phase to be between 1573 and 1623 K in a steel containing larger amounts of niobium and nitrogen.

Robinson and Jack[22] report the formation of Z phase in a 20Cr–9Ni steel containing 0·38 wt-%N and 0·27 wt-%Nb between 700 and 1000°C. At 1000°C, Z phase is the first and only phase formed. It is found uniformly distributed after 30 min but coarsens rapidly. At 700°C it starts to precipitate in the matrix after 16 h. At lower temperatures, Vodárek[23] reports a considerable dimensional stability of Z phase in a type 316LN alloy, with a mean size of 6 nm after 82 h at 650°C and 12 nm after 37 890 h at the same temperature.

Thorvaldsson and Dunlop,[24] studying the effects of stabilising elements in austenitic stainless steels, use an 18–12 steel with 0·4 at.-%V, 0·13 at.-%Nb, and 0·43 at.-%N. After 5000 h at 750°C, no Z phase has formed, but a (Nb,V)(C,N) fcc carbonitride forms instead. Andrén *et al.*,[14] with the same composition in very similar conditions, found, in contrast, that the MX precipitate always had a stoichiometry not far from $MX_{0{\cdot}5}$, and contained appreciably as much chromium as (Nb+V). However, the characteristic tetragonality was not observed and the authors suggested that they had found a precursory state of the fully ordered Z phase.

Considerations on stability of Z phase

It seems fairly reasonable to propose that Z phase is the stable niobium containing phase in austenitic stainless steels with a high nitrogen content. Hughes[13] suggests that it can be expected in a typical 347 steel as soon as the amount of nitrogen is greater than 0·06 wt-%. Knowles[25] finds Z phase in a 20–25 0·41 wt-%Nb steel with 0·028 wt-%N, which could indicate that the chromium and/or nickel content plays an important role in the solubility of this phase.

The problem arises, in many steels, to know whether NbC or Z phase is the more stable. Very few studies have dealt with additions of Nb, C, and N together in a way that could determine which phase is more stable, often niobium is in excess and both NbC and CrNbN form. Uno *et al.*[26] found that only Z phase formed in an 18–12 niobium stabilised steel with carbon and nitrogen, the niobium content being lower than that required to combine either all carbon or all nitrogen. This would indicate that Z phase is fast enough to form first when competition between NbC and CrNbN is likely to occur. On the other hand, Knowles[25] reported Nb(C,N) after 2 h at 850°C in a 20–25 steel, transforming to Z phase with further aging. From the precipitation behaviour of NF709,[5] where Z phase is reported after aging times of 10^4 h at 750°C, and carbon containing phases are $M_{23}C_6$ and M_6C, it can be inferred that Z phase is more stable than NbC and that the latter will dissolve in preference to the former if niobium is in too small quantities. However, Raghavan *et al.*[21] deduce from a comparison between types 347 (18–12 with 0·8 wt-%Nb and 0·07 wt-%C) and 347AP (18–12 with 0·3 wt-%Nb, 0·09 wt-%N, 0·009 wt-%C) a greater stability of NbC, since Z phase is found to precipitate from the solid state but the NbC is found as residual particles. The conclusions of such a comparison must be examined carefully as the steel compositions were different.

Conclusions about Z phase

Generally, it can be concluded that Z phase precipitation is not fully understood. Points of agreement are its stability at high temperature and the features of its precipitation (fine dispersion); proposed solvus temperatures differ between studies, but these differences are consistent with different compositions. It is difficult as yet to build a coherent view of the various kinetics observed. It is not clear whether Z phase actually forms from MX precipitates as suggested by the results of Knowles[25] and Andrén *et al.*,[14] or directly as suggested by Robinson and Jack.[22] These observations may be reconciled if it could be proved that the driving force in a 20Cr–10Ni alloy[22] is significantly different from that in an 18–12 alloy. The importance of Z phase in both ferritic and austenitic power plant steels renders particularly necessary the assessment of the ternary system Cr–Nb–N, to provide the thermodynamic parameters required for any prediction.

$M_{23}C_6$

Structure and composition

The term $M_{23}C_6$ is a more general notation for $Cr_{23}C_6$, as often, Ni, Mo, and Fe are found to substitute partially for chromium. It is the main carbide in non-stabilised carbon containing austenitic stainless steels; nitrogen bearing steels form Cr_2N. It has a fcc structure (and space group *Fm3m*) of lattice parameter varying between 1·057 and 1·068 nm, which is about three times that of the austenite. It is often reported to grow with a cube to cube orientation relationship

$$\{100\}_\gamma \| \{100\}_{M_{23}C_6}$$

$$\langle 010 \rangle_\gamma \| \langle 010 \rangle_{M_{23}C_6}$$

It is in most cases the main carbide found in austenitic stainless steels. Although $M_{23}C_6$ can be only metastable, it is always found in the early stage of precipitation because it nucleates very easily.

Morphologies and locations

The phase $M_{23}C_6$ is mainly reported to precipitate on the following nucleation sites, and in this order: grain boundaries, incoherent and coherent twin boundaries, intragranular sites. In niobium stabilised grades, it is sometimes reported to nucleate on undissolved (i.e. during the solution treatment) niobium carbonitrides. Generally, $M_{23}C_6$ shows only {111} and {110} interface planes. This has been explained by Beckitt and Clarck,[27] who showed that these planes have the best atomic correspondence with the austenite.

Precipitation on grain boundaries The precipitation of $M_{23}C_6$ has been the focus of many investigations, motivated by its importance in terms of corrosion resistance. On grain boundaries $M_{23}C_6$ is often associated with intergranular corrosion. It is found after very short aging times (30 min at 750°C (Ref. 28), even in stabilised steels. It causes the grain boundary to move, and therefore shows on one side, the new grain boundary, while the other has a serrated aspect composed of the {111} interfaces. These precipitates are usually large (Fig. 3). When boron is added, the number density of $M_{23}C_6$ along the grain boundaries increases,[30] with beneficial effect for the creep rupture strength, as the grain boundary sliding and surface cracking are reduced. Other effects of boron in $M_{23}C_6$ are dealt with below.

Precipitation on incoherent and coherent twin boundaries On incoherent and coherent twin boundaries, $M_{23}C_6$ forms long plates parallel to the twin boundaries (Fig. 4*a*). The plates are, as for any form of $M_{23}C_6$ in austenitic stainless steels, bounded by {110} and {111} planes only. The large faces are {111} planes parallel to the twin boundaries. Plates grow initially from the incoherent twin boundary, but some are found later apparently detached from the boundary. Precipitation on the coherent boundary occurs more slowly than on incoherent boundaries. The mechanism of their formation has been the subject of controversy. Beckitt and Clarck[27] suggested that carbides growing on the incoherent twin boundary repel Shockley partial dislocations in the twin, and these cause nucleation of new plates in the twin. However, detailed observations have led Singhal and Martin[31] to conclude the stacking faults grew first in the twin; $M_{23}C_6$ would then nucleate on the Shockley bounding dislocation and grow in the stacking fault, possibly helped by an enrichment of this stacking fault in chromium. Both fail to explain why these plates are usually separated from the boundary and from each other (according to these mechanisms, they should be connected to the incoherent twin boundary by a stacking fault). Another mechanism has been proposed more recently by Sasmal.[32] Noting that plates do not form away from the boundary or on coherent twin boundaries if specimens are held at the aging temperature directly after the solution treatment, Sasmal suggested that the formation of plates of $M_{23}C_6$ close to but detached from the incoherent twin boundaries, and on coherent boundaries, was an effect of residual stress developed in these regions. It could be argued here that stress only influences the formation: if it favours the formation of $M_{23}C_6$ plates parallel to the twin boundaries, there should still be a small percentage of plates growing along other equivalent orientations.

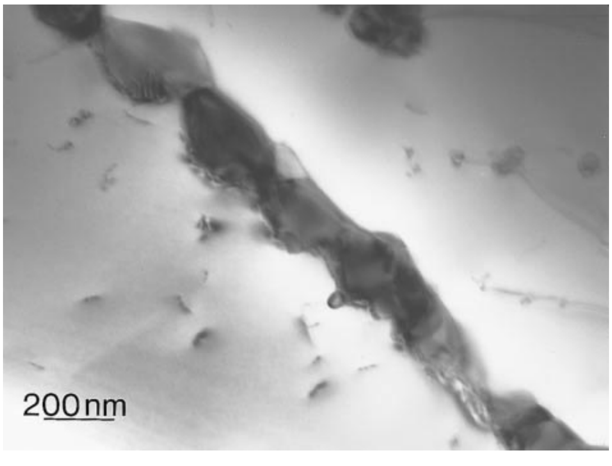

3 Precipitate $M_{23}C_6$ on grain boundary[29]

Intragranular precipitation In the austenite grains, $M_{23}C_6$ precipitates as cuboids or plates. The latter have the same characteristics as the plates growing from twin boundaries (*see* Fig. 4*a*). The cuboids grow on dislocations until they form a continuous chain sharing their corners. These chains can form branches, leading to secondary stringers of $M_{23}C_6$. Beckitt and Clarck[27] have proposed a satisfactory explanation for the formation of these secondary stringers: the growth of primary $M_{23}C_6$ generates dislocations on which other precipitation can occur. The orientation of these secondary stringers is that expected by this mechanism. i.e. the normal orientation of edge dislocations in austenite.

Another kind of intragranular precipitation has been reported by Sasmal.[33] Plates of $M_{23}C_6$ can form around undissolved niobium carbonitrides in niobium stabilised steels (Fig. 4*b*). In this case, the large faces are {110} and the edges are {111}. The reasons for this change are not clear, although a contribution of the strain around the undissolved particle is invoked.

Role of other alloying elements

Initially, $M_{23}C_6$ is a Cr–Fe carbide. However, its composition is susceptible to large variations. For example, in a typical 2·25Cr–1Mo steel, $M_{23}C_6$ has a composition of ~0·3Fe–0·38Cr–0·1Mo–0·22C (mole fraction), while in a typical 304 steel, it is closer to 0·04Fe–0·65Cr–0·11Mo–0·22C. There is also evidence that, for a given steel composition, the $M_{23}C_6$ composition undergoes large changes in the early stages of precipitation. Lewis and Hattersley[28] quote a study by Philibert *et al.*[34] in which the authors propose that M_7C_3 forms in the early stages of aging in an 18–8 steel, as the Fe/Cr ratio is more consistent with the known composition of this phase. Similarly, Marshall[4] quotes a study[35] in which the authors show that up to 40 wt-%Fe can be found in $M_{23}C_6$ in the early stages of precipitation, but also that the molybdenum content increases with time. It is proposed by the present author that these composition changes can be explained by the growth mechanism involved. In a multicomponent alloy, the interface has to move at a rate consistent with the flux of each element, to maintain local equilibrium. Therefore, the interfacial compositions are not in general given by a tie line passing through the bulk composition, but by an alternative tie line which permits the flux balance (details are outside the scope of the present review; *see*, for example, Ref. 36 or 37).

In the same way, on the interstitial lattice, boron can substitute for carbon, albeit both in very small quantities. Boron is of particular interest as it promotes the formation of intragranular $M_{23}(C,B)_6$. There is some controversy

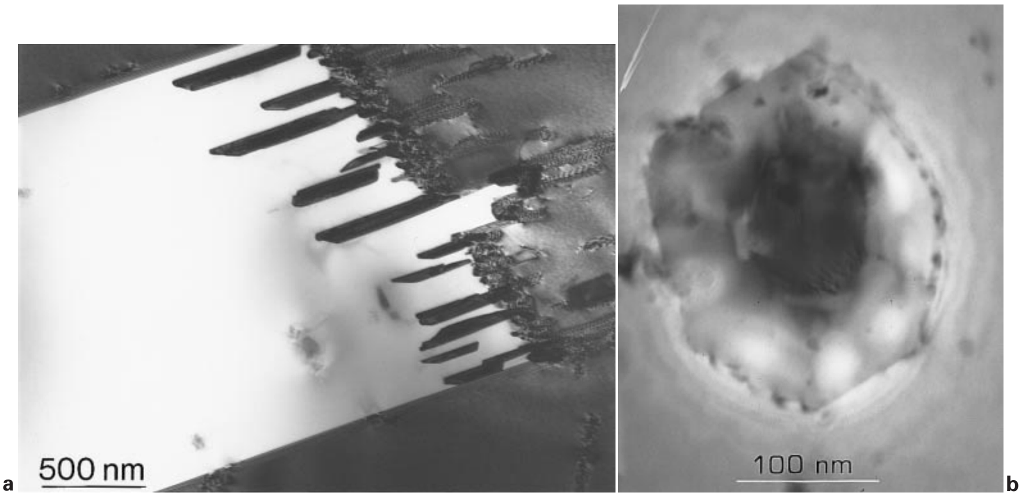

4 Plates of $M_{23}C_6$ growing *a* from incoherent twin boundary and *b* around Nb(C,N) precipitate[29]

about the mechanism involved, but it is possible that boron increases the lattice parameter of $M_{23}C_6$, therefore reducing the mismatch with the austenite. The presence of boron in $M_{23}C_6$ has been demonstrated using atom probe field ion microscopy (APFIM; for example, Ref. 38). The same is not true for nitrogen. It has long been believed to have a small solubility in $M_{23}C_6$ (for example, Ref. 39). However, recent experimental results supported by *ab initio* calculations indicate zero solubility of nitrogen in $M_{23}C_6$, the structure of which is destabilised if a small amount of carbon is replaced by nitrogen.[8]

Except in the fine intragranular form, $M_{23}C_6$ precipitation is not desirable for good creep properties. It is often associated with intergranular corrosion, as its formation along the grain boundaries causes a local depletion in chromium and possibly local loss of the stainless property (the steel is then said to be sensitised, i.e. susceptible to intergranular corrosion).

Solubility and kinetics of precipitation

The solubility of carbon in austenite, with regard to $M_{23}C_6$, has been described by empirical relationships such as[40]

$$\log[\mathrm{C}]_{\mathrm{ppm}} = 7{\cdot}71 - \frac{6272}{T}$$

As can be seen in Fig. 5, this is valid for a typical 18–12 steel, but care should be exercised as the solubility of carbon is appreciably modified by the chromium and nickel content. Increasing the chromium content reduces the solubility of carbon in austenite. It also increases the kinetics of $M_{23}C_6$ precipitation, as does an increase in carbon content: from 0·02 to 0·08 wt-%C, the nose of the C curve is shifted from 100 to 0·1 h.

At first $M_{23}C_6$ precipitates on grain boundaries, then, with increasing time, on incoherent twin boundaries, coherent twin boundaries, and finally in the matrix on dislocations. In the matrix, it forms as evenly spaced angular blocks. At long aging times, grain boundary carbides can form a completely interlocked structure.

The kinetics of precipitation is affected by molybdenum, which stabilises the carbide and accelerates its formation. On the other hand, nitrogen is well known to retard both formation and coarsening rates of $M_{23}C_6$, and an often proposed explanation is that nitrogen reduces the diffusivities of chromium and carbon in the austenite.[4,9] However, Degalaix and Foct[41] found that if the carbon content was higher than 0·08 wt-%, increasing the nitrogen content could have the opposite effect. More recent investigations indicate that nitrogen actually enhances the diffusion of substitutional elements by increasing the formation of vacancies, but delays the nucleation of $M_{23}C_6$, the structure of which is destabilised when carbon is partially substituted by nitrogen.[8]

Relative stability of $M_{23}C_6$

In a simple type 304 steel, $M_{23}C_6$ is often the only carbide found at any aging time. Although sometimes M_6C is found,[42] it is as a minor phase and no mention is made of an instability of $M_{23}C_6$ with regard to M_6C. When molybdenum is added (type 316), $M_{23}C_6$ can partially transform to M_6C (*see* below); it is however always reported that $M_{23}C_6$ remains the main carbide even after long aging. In fact, $M_{23}C_6$ and M_6C also coexist in the steel X5CrNiMo1713 (17Cr–13Ni–5Mo (wt-%)) studied by Thier *et al.*[43] This is not the case when niobium is involved in the formation of M_6C, which seems then more stable and becomes the dominant carbide at long aging times.[44]

In stabilised grades, the situation is much more complex. From the literature found, it is not possible to state clearly whether $M_{23}C_6$ is sometimes formed first or always follows MX precipitation, nor which phase is the more stable on long term aging.

Thorvaldsson and Dunlop,[24,45,46] studying the effect of various stabilising elements and their combinations, found

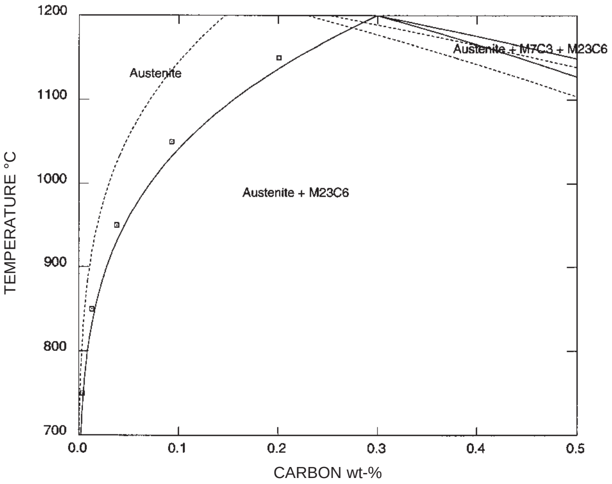

5 Solubility of C in austenite with regard to $M_{23}C_6$ precipitation, calculated using MTDATA, allowing for austenite, $M_{23}C_6$, M_7C_3, and liquid with elements Fe, Cr, Ni, 0·3Si, and 1·0Mn (wt-%): solid lines for 18–12 and broken lines for 20–25 steel, squares correspond to empirical relationship[40]

that $M_{23}C_6$ was more stable than TiC, but less than NbC. This is consistent with the results of Grot and Spruiell,[47] who found formation of $M_{23}C_6$ in a type 321 steel after long term aging, and with the results of Kikuchi *et al.*[9] for a 20–25 steel. These authors concluded that TiC retards the precipitation of $M_{23}C_6$ but does not suppress it.

On the other hand, Bentley and Leitnaker,[48] studying a type 321 steel that had been in service for 17 years at 600°C, did not find any $M_{23}C_6$, and concluded that TiC was more stable. Lai[49] observed no $M_{23}C_6$ in a type 321 steel used up to rupture (16 000–29 000 h at 600°C).

Obviously, consideration of the relative stabilities of the two phases makes sense only if the titanium content is sufficient to combine all carbon present, as, in the opposite case, $M_{23}C_6$ forms with the excess carbon. The studies in which $M_{23}C_6$ formation appears as an anomaly deal with steels in which the titanium content is higher than or equal to that required for full stabilisation.

The agreement is better for NbC, which is more stable than $M_{23}C_6$. However, $M_{23}C_6$ can form as a transient phase.

M_6C

The phase M_6C is also known as η carbide, but is referred to as M_6C to avoid confusion with η phase (Laves phase). It generally describes a phase of very variable composition. In most cases, it is formed only after long aging times, and therefore is relatively little documented. Moreover, its appearance and disappearance are strongly linked to that of other constituents, and it is difficult to allocate it any absolute location in a time–temperature precipitation (TTP) diagram.

Structure and composition

The structure of M_6C is diamond type fcc carbide, with a lattice parameter varying between 1·095 and 1·128 nm. Its space group is *Fd3m*, distinguishing it from $M_{23}C_6$ and G phase which both have fcc structures with similar lattice parameters but an *Fm3m* space group. The η carbide structure is described by Stadelmaier in Ref. 50, for example. This structure encompasses a wide range of compositions, and only those commonly found in creep resistant austenitic stainless steels are reviewed here.

The composition of M_6C can be molybdenum rich ($(FeCr)_{21}Mo_3C_6$) or niobium rich (Fe_3Nb_3C). The molybdenum rich Fe_3Mo_3C ($a = 1{\cdot}111$ nm) was reported in high molybdenum steels, but never in austenitic steels.[51] Instead, a fraction of molybdenum is replaced by iron or chromium, and the lattice parameter is reduced ($a = 1{\cdot}095$ nm).[51] The composition reported by Brun *et al.*[52] in a 316 steel containing titanium shows substantial amounts of nickel also dissolving in M_6C: 4·5Si–6·5Mo–0·8Ti–30Cr–0·5Mn–26·7Fe–31Ni (at.-%).

Silicon has been reported to dissolve in this phase to form M_5SiC, but such a phase is very seldom found. Other elements that can be included in the general notation M are Ni, Ti, and Co. In NF709 (a 20–25 niobium stabilised alloy, with 0·17 wt-%N), long term aging allows formation of Cr_3Ni_2SiC; such a composition has been reported by Williams[53] in a study of irradiated type 316 and by Titchmarsh and Williams[54] in a similar steel, at rather low temperatures (466°C) but not above 670°C. Its formation in such steels is linked with the segregation effects caused by irradiation, in particular the segregation of silicon to point defect sinks. This particular composition has a lattice parameter of 1·062 nm (JCPDS 17-330), which makes it extremely similar to $M_{23}C_6$ from a structural point of view. Although always referred to as Cr_3Ni_2SiC, its actual composition includes substantial amounts of molybdenum and iron (*see* Table 4), the concentrations of which increase with temperature.[53] Williams therefore proposed the more general formula $(Cr,Mo)_3(Ni,Fe)_2SiC$.

Jargelius-Petterson[55] found a nitrogen rich similar phase (Cr_3Ni_2SiN) after furnace aging of a 20Cr–25Ni–5Mo–0·2N steel. It is reported after both 5 and 3000 h at 850°C, and therefore is probably an equilibrium phase. In agreement with the observation that the molybdenum content increases with temperature, the composition found in this case includes as much as 25 wt-%Mo (also a result of the larger molybdenum content of the alloy).

Occurrence and stability

Mo rich compositions In a type 316 steel, the composition of M_6C is close to $(FeCr)_{21}Mo_3C_6$. Weiss and Stickler[51] proposed that it formed according to

$$M_{23}C_6 \rightarrow (FeCr)_{21}Mo_3C_6 \rightarrow M_6C$$

It is not reported by Minami *et al.*[44] after 10 000 h at 750°C (instead, χ phase is found), nor by Lai and Meshkat[56] after 10 000 h at 600 and 650°C, nor by Barcik[57] for the same aging time, up to 900°C. However, it was found by Stoter[58] in specimens of 316 steel that had been in service at 650°C for 28 000 and 60 000 h, in very small amounts and always associated with $M_{23}C_6$.

Nitrogen seems to have a large influence on M_6C formation. Thier *et al.*[43] did not find this carbide after 1000 h in a type 316 steel with 0·037 wt-%N, but found it after only 1 h aging at 900°C when the nitrogen content was 0·069 wt-%. Gavriljuk and Berns[8] suggest that the calculations performed by Jargelius-Petterson[59] raise controversy, as she shows that an increase of nitrogen in a 20Cr–25Ni–4·5Mo (wt-%) steel reduces the driving force for M_6C formation.

However, it must be noted that M_6C is rather poorly described in the SGTE databases, as these contain information about only the molybdenum rich carbide; that is to say they describe only one of the possible compositions of the η structure. In this regard, it is possible to say that the η structure is in both cases stabilised, but with different compositions. In particular, Jargelius-Petterson[59] reports that M_5SiN is always present and favoured by high nitrogen contents. It seems, therefore, that nitrogen generally stabilises the η structure, but the composition of this phase varies with the alloy.

For type 321 steel (titanium stabilised), none of the studies found in the literature report M_6C.

Nb rich compositions In type 347 steel, in contrast, the presence of niobium seems to promote the formation of a niobium rich M_6C. Care should be taken as Powell *et al.*[60] argue appreciably that G phase and M_6C have often been confused. However, if the structures are very

Table 4 Some compositions of Cr_3Ni_2SiC in irradiated 316 steel, at.-% (Ref. 53)

Temperature, °C	Cr	Mo	Si	Ni	Fe
500	35	11	20	24	10
600	32	15	20	24	10

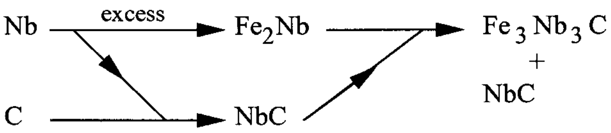

6 Precipitation sequence leading to M_6C when Nb is in excess, as proposed by Minami *et al.*[61]

similar, the composition should clearly differentiate Fe_3Nb_3C or Cr_3Ni_2SiC (as in NF709) from $Ni_{16}Nb_6Si_7$. The experimental methods must be linked with the results of the various studies. In general, niobium rich M_6C seems to form only on long term aging. Kikuchi *et al.*[9] do not report it after 1000 h at 700°C in a 20–25 steel. In an 18–8 steel, it is reported between 600 and 800°C by Minami *et al.*[44] at very long aging (~50 000 h) for 600°C but soon (~2000 h) for 800°C. They propose a sequence illustrated in Fig. 6.[61] This mechanism implies that excess niobium is present. If niobium is less than that required for combination of all carbon, no such phase is observed (steel Tempaloy-A1 in Ref. 44, similar to a type 304 with 0·13Nb–0·06Ti–0·07C (wt-%)).

In 20–25 alloys, as suggested above, M_6C and G phase have probably often been confused (for example, Ref. 62) in early studies where identification relied on X-ray or electron diffraction only. It is difficult to conclude which phase forms preferentially. Ramaswamy and West[63] report M_6C in a 20–25 steel with low silicon content (0·03 wt-%), but other studies report G phase (alloy silicon content 0·4–0·7 wt-%).

When nitrogen is present (in 347 or 20–25 steel) in sufficient quantities, Z phase forms and it is difficult to determine its stability relative to M_6C.

Cr_3Ni_2SiX and G phase The G phase, which is considered further below, is an alternative silicon rich phase to Cr_3Ni_2SiC. As mentioned above, the composition Cr_3Ni_2SiC is very seldom reported in the literature. Titchmarsh and Williams have reported its formation in irradiated steel of composition close to that of 316 with the addition of 1·8 wt-%Nb. They noted[54] and provided evidence[64] that G phase formed preferentially only when carbon was not available.

In 20–25 niobium and carbon containing steels, however, Powell *et al.*[60,65] and Ecob *et al.*[66] have found G phase and observed that NbC partially transforms to G phase with time. It seems reasonable to propose that, in 20–25 steel, G phase is stabilised with regard to Cr_3Ni_2SiC, probably because of the larger nickel content.

However, in NF709 (Ref. 5, composition given in Table 1), Cr_3Ni_2SiC is reported. This is inconsistent with the studies quoted above which seem to indicate G phase to be the more stable phase. It is not clear whether the presence of carbon or nitrogen was investigated or the composition Cr_3Ni_2SiC was assumed. Investigations of the exact nature of this precipitate are required to determine whether it is a nitride or a carbide. A nitride would be expected, as it would not be incoherent with the above observations that G phase is more stable than Cr_3Ni_2SiC and that the η structure is stabilised by nitrogen.

Intermetallic phases

σ PHASE

This is a well known intermetallic phase which forms in the Fe–Cr system, with composition FeCr. In highly alloyed steels, its composition is variable. Its precipitation is associated with embrittlement. In creep resistant steels, σ phase has a detrimental effect on creep properties when precipitated on grain boundaries, but little effect when it precipitates intragranularly.

Structure and composition

The σ phase has a tetragonal unit cell (space group $P4_2/mnm$) with $a=0{\cdot}880$ nm and $c=0{\cdot}454$ nm (FeCr). This unit cell contains 30 atoms. Reported orientation relationships are[4]

$$(111)_\gamma \| (001)_\sigma$$

$$(0\bar{1}1)_\gamma \| (140)_\sigma$$

or

$$(111)_\gamma \| (001)_\sigma$$

$$(\bar{1}10)_\gamma \| (\bar{1}10)_\sigma$$

The composition varies fairly widely and it is difficult to give a formula. For example, Jargelius-Petterson[59] reports the following range of composition (wt-%) for σ in a 20–25 steel with molybdenum content varying between 4·5 and 6·0 wt-%: (35–43)Fe–(0–1)Si–(1–9)Mn–(27–32)Cr–(10–16)Mo–(8–15)Ni. For a type 316 steel,[39] a typical composition is (wt-%, other elements not given) 44Fe–29·2Cr–8·3Mo.

Occurrence

An in depth review of σ phase precipitation in Cr–Ni austenitic steels has been done by Barcik.[67] The phase precipitates first on triple points then on grain faces. After long term aging at high temperature (10 000–15 000 h at 873 K), it also forms on incoherent twin boundaries and intragranular inclusions. The mechanism of nucleation is still a matter of controversy, particularly regarding the role of δ ferrite and $M_{23}C_6$ in the nucleation process. Studies have reported its formation associated with the dissolution of $M_{23}C_6$, but also independently.[4] It is found in most grades of austenitic stainless steel: types 304, 316 (Mo), 321 (Ti stabilised), and 347 (Nb stabilised) (*see*, for example, Ref. 44). However, it forms after different times. The 25Cr–20Ni steels can exhibit as much as 20 wt-% of σ phase.

In stabilised grades, its formation is faster than in other grades. Minami *et al.*[44] report precipitation of σ after 1000 h at 700°C in types 347 and 321 (347 precipitating σ slightly faster than 321). In 304, 316, and Tempaloy-A1, σ phase is found in significant quantities only after 10 000 h (Fig. 7). It is worth noting that Tempaloy-A1 is niobium stabilised, but with a Nb/C ratio of 1·86, while this ratio is 17·40 in the 347 steel. This correlates well with the fact that σ forms when the carbon content falls below a critical value when the chromium equivalent is higher than 18 wt-%. In type 347, almost all the carbon is rapidly precipitated as NbC, while the low niobium content of Tempaloy-A1 leaves some carbon in solution. The different trend for 321 steel

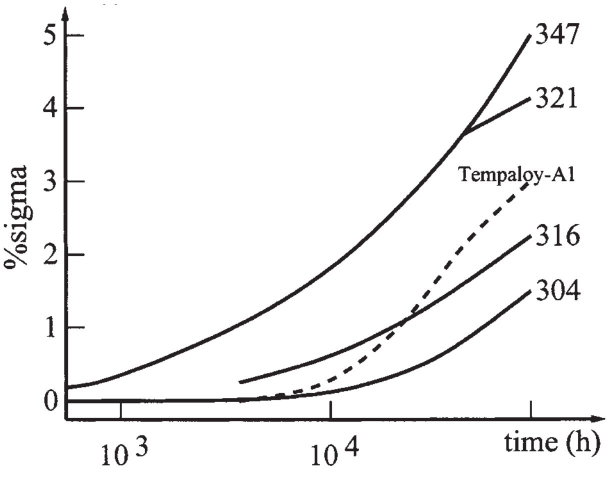

7 Precipitation of σ in different grades of austenitic stainless steel at 700°C: Tempaloy-A1 is 18–10 steel with Nb/C ratio of 1·86, whereas 347 steel has ratio of 17·40; percentage is area etched by KOH (Ref. 44)

could be linked to the instability of TiC with regard to $M_{23}C_6$. The precipitation of $M_{23}C_6$ lowers both the carbon and the chromium contents. The results of Grot and Spruiell[47] show in contrast no σ phase formation at up to 2000 h in a type 321. The σ phase is also found in 20–25 (Fig. 8). Various factors affect the formation of σ phase. Elements such as Cr, Nb, Ti, and Mo are known to promote σ formation. Silicon promotes and accelerates its formation. In general, the formation of σ in austenite is about 100 times slower than in ferrite. Consequently, the presence of δ ferrite accelerates σ precipitation.[67]

A method has been developed by Woodyatt *et al.*[68] to estimate the σ forming tendency of an alloy, based on the electron vacancy number $\bar{N}_v$

$$\bar{N}_v = 0{\cdot}66[\mathrm{Ni}] + 1{\cdot}71[\mathrm{Co}] + 2{\cdot}66[\mathrm{Fe}] + 4{\cdot}66[\mathrm{Cr} + \mathrm{Mo} + \mathrm{W}] + 5{\cdot}66[\mathrm{V}] + 6{\cdot}66[\mathrm{Zr}] + 10{\cdot}66[\mathrm{Nb}] \quad (\text{at.-\%})$$

If the value of $\bar{N}_v$ is higher than 2·52, the alloy should form σ.

LAVES PHASE

Laves phase is found in various grades of austenitic stainless steel. It is often a minor constituent. It precipitates intragranularly in the form of equiaxed particles, occasionally on grain boundaries.[51] Whether or not Laves phase has a detrimental effect on creep properties is still discussed. In niobium stabilised steels, however, it is likely that Laves phase is detrimental because it allows the formation of M_6C (*see* below).

Structure and composition

Laves phase is a hexagonal phase of space group *P6₃/mmc*, with $a = 0{\cdot}473$ nm and $c = 0{\cdot}772$ nm. As the main factor determining its formation is the relative atomic size of the constituent atoms, the ranges of composition are fairly small. Jargelius-Petterson[59] measured the composition of Laves phase in a 20–25 alloy with 5 wt-%Mo, and the results are given in Table 5. This shows that Laves phase probably does not form at its exact equilibrium composition. In stabilised grades, Fe_2Nb or Fe_2Ti (more seldom) can form.

Denham and Silcock[69] proposed for Fe_2Nb the following orientation relationships

$$(0001)_{\mathrm{Fe_2Nb}} \| (111)_\gamma$$

$$(10\bar{1}0)_{\mathrm{Fe_2Nb}} \| (\bar{1}10)_\gamma$$

Occurrence

In type 304 steel, Laves phase is not found, owing to the absence of Mo, Nb, or Ti. In type 316, which contains typically 2–2·5 wt-%Mo, it is found after relatively long aging times. Minami *et al.*[44] report its formation after a minimum of 1000 h, between 625 and 800°C. The experimental results of Lai[70] are in agreement with the dissolution of Fe_2Mo above 800°C. Coherently, White and Le May[71] do not report any Laves phase precipitation between 640 and 800°C for aging times up to 900 h. Weiss and Stickler[51] report a slightly higher maximum temperature for Laves precipitation in type 316, as they found it up to 815°C. Its formation interacts in a competitive way with that of σ and χ phases. For example, the presence of δ ferrite delays its formation because it enhances that of the σ and χ phases.

In titanium stabilised grades, the formation of Fe_2Ti is never reported in compositions similar to that of a 321 steel. Minami *et al.*[44] do not report it for aging times up to 50 000 h between 600 and 750°C, in a type 321 steel. However, it is found by Beattie and Hagel[72] in an A286 type alloy, containing 16 wt-%Cr, 26 wt-%Ni, and 1·8 wt-%Ti, after 1000 h at 815°C. This is directly related to the large amount of titanium used in such steels, compared with a typical 321 alloy.

In niobium stabilised steels, Fe_2Nb is frequently reported after long aging times, but as a transient phase which disappears when Fe_3Nb_3C forms. It is reported to form in a type 347 with 0·87 wt-%Nb and 0·05 wt-%C, after 1000 h between 650 and 800°C, and to disappear after 5000–10 000 h.[44] However, its formation is dependent on the availability of niobium. In the same study, the Tempaloy-A1 (18–10 with 0·13 wt-%Nb for 0·07 wt-%C) does not precipitate Laves phase after aging treatments of up to 25 000 h. Instead, only NbC is found (*see* Fig. 6). The same results are reported by Raghavan *et al.*,[21] who found NbC and Laves phase in a type 347 steel with 0·8 wt-%Nb and 0·07 wt-%C (8000 h at ~600°C), but only Z phase in a modified 347 with 0·3 wt-%Nb and 0·09 wt-%N. It is therefore probable that both NbC and Z phase are more stable than Fe_2Nb.

χ PHASE

This is, most of the time, a minor intermetallic phase. It is mainly found in type 316 steel above 750°C.

Structure and composition

The χ phase is a body centred cubic (bcc) phase of space group *I4̄3m*. The unit cell contains 58 atoms and has a lattice parameter varying between 0·8807 and 0·8878 nm. A typical composition is $Fe_{36}Cr_{12}Mo_{10}$, but the phase has a high tolerance for metal interchanges. The crystal structure has large interstices which allow the presence of carbon, sometimes making this phase better described as a $M_{18}C$ carbide. It nucleates on grain boundaries and incoherent twin boundaries, but also intragranularly on dislocations.

Occurrence

Although it is sometimes (but seldom) present in very small quantities in 321 steel,[44] χ phase is a significant phase only in type 316, when the aging temperature is high enough. For example, it is reported by Minami *et al.*[44] for times up to 25 000 h and temperatures between 700 and 850°C, and by Lai[70] as the main phase with σ between 715 and 850°C for times up to 5000 h, but not by Stoter[58] after 28 000 and 60 000 h at 650°C.

G PHASE

The G phase is a silicide forming in austenitic stainless steels stabilised with titanium or niobium. It was first reported by Beattie and Versnyder[73] in 1956 in an A286 type steel, that is a precipitation hardening 26Ni–15Cr alloy with variable (0–2·3 wt-%) titanium and aluminium contents. It has long been believed to form only under irradiation in steels of the 300 series and in 20–25 steels. However, Powell *et al.*[60] showed in 1988 that it formed under normal aging in 20–25 niobium stabilised alloys, in the temperature range

Table 5 Compositions of Laves phase, wt-% (Ref. 59)

	Fe	Mo	Cr	Ni	Mn	Si
After 10 min at 850°C	29±2	36±2	19±2	13±1	1·5±0·8	1·8±0·5
After 3000 h at 850°C	37±1	35±1	12±1	14±1	~0	0·7±0·2

500–850°C, and suggested that it had been identified as M_6C in earlier studies of the same steel.

Structure and composition

The G phase has a general formula $A_{16}D_6C_7$, where A and D are transition elements, and C is a group IV element;[66] A is usually nickel, and D is usually niobium[60,65,66] or titanium.[49] Ecob *et al.*[66] mentioned the possibility of substitution, in small quantities, of D (i.e. niobium or titanium) by iron or chromium, and Powell *et al.*[60] measured the following composition: 51Ni–29Nb–14Si–4·5Fe–1·5Cr (wt-%).

Lai[49] found a titanium containing G phase in a type 321 steel, and gives a composition appreciably richer in nickel: 63·3Ni–20·9Ti–12·2Si–3·47Fe–0·13Cr (wt-%). Note that neither of these compositions clearly shows substitution of D when trying to match the stoichiometric formula.

The G phase has a fcc structure with a lattice parameter of 1·12 nm; this corresponds to a content of 116 atoms per unit cell. The space group for this structure is *Fm3m*. It is remarkable that the lattice parameter seems to be the same for $Ni_{16}Nb_6Si_7$ (*see* Refs. 60 and 65) and $Ni_{16}Ti_6Si_7$ (*see* Refs. 49 and 72). In an earlier study, Sumerling and Nutting,[62] studying a 20–25 niobium stabilised steel, found a lattice parameter of $1·125 \pm 0·005$ nm for a phase they identified as M_6C.

As mentioned above, Powell *et al.*[60] have suggested that G phase was identified as M_6C in early work on 20–25 niobium stabilised steels because of their similar compositions and structures. A detailed investigation of the structure is sufficient to solve the problem,[66] but additional evidence has been sought by the use of electron energy loss spectroscopy (EELS) (as in Ref. 60) or a wavelength dispersive crystal spectrometer in SEM (as in Ref. 49), both techniques making possible quantitative measurements of light elements (C, N). These studies have confirmed the absence of interstitial elements in G phase.

Occurrence of G phase in austenitic stainless steels

The general features of G phase formation are:

(i) it forms very predominantly on grain boundaries (hence its name)
(ii) it is now clear that it forms in 20–25 niobium stabilised steels and to an extent that depends on the silicon content
(iii) it has also been reported in a type 321 steel, but other results are contradictory.

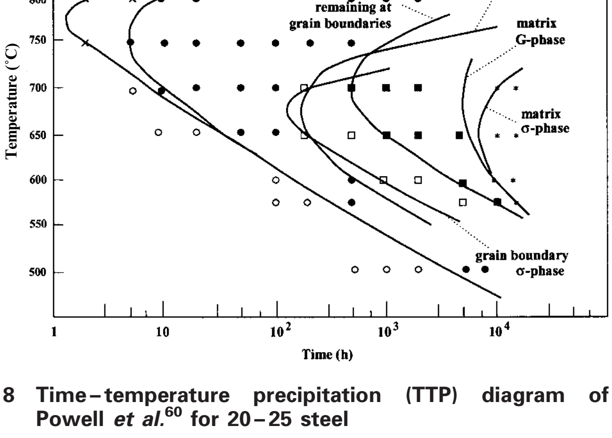

8 Time–temperature precipitation (TTP) diagram of Powell *et al.*[60] for 20–25 steel

Ti rich G phase In one of the first studies of G phase,[72] the titanium rich G phase is reported in an A286 type steel. It is not clear for what conditions of temperature and time it forms, as it was often found to resist the solution treatment. However, G phase was not found in the alloy containing only 0·01 wt-%Si, but formed at higher contents, and the volume increased with an increase in silicon content. Adding 2 wt-% of aluminium suppressed the formation of G phase. This work also included a steel in which the titanium content is more like that used in the 300 series, and no G phase was found.

The only report found of titanium rich G phase in type 321 steel is quoted above.[49] Three of seven type 321 steels show G phase after 16 000 and 50 000 h at 600°C. The common factors in the three type 321 steels found to form titanium rich G phase in this study are their small grain sizes and an excess of titanium with regard to the amount of carbon present. However, under similar conditions, other studies[44,48] do not report G phase.

Nb rich G phase In 20–25 niobium and carbon stabilised steels, it is now clear that G phase can form (*see* Refs. 60, 65, and 66) and, following the suggestion of Powell *et al.*[60] the works of Sumerling and Nutting[62] and Dewey *et al.*[74] may be regarded as other evidence for G phase formation if it is accepted that M_6C must be interpreted as G phase. In Ref. 62, in particular, the authors measured a lattice parameter of $1·125 \pm 0·005$ nm, which is much closer to the G phase parameter.

Powell *et al.*[60] summarised their work in a TTP diagram as shown in Fig. 8. In their alloy (0·68 wt-%Nb, 0·037 wt-%C, 0·61 wt-%Si), G phase forms between 500 and 850°C, first on residual grain boundary particles of NbC, and only after very long aging on NbC particles in the matrix. The authors propose that this is because of the easier diffusion of required elements in the grain boundaries.

Ecob *et al.*,[66] comparing the occurrence of G phase in similar 20–25 niobium stabilised steels, noticed that alloys apparently similar in composition exhibited different relative stabilities of NbC with regard to the G phase. They found that an increase in the oxygen content led to a greater instability of NbC relative to G phase, and proposed that oxygen and silicon are involved in a cosegregation process, a greater amount of oxygen segregating around NbC leading to a greater segregation of silicon in the same way. The silicon rich region is more favourable to G phase formation.

In 20–25 niobium and nitrogen containing steels, however, as discussed in the above section regarding M_6C, it seems that Cr_3Ni_2SiN forms preferentially to G phase. No results could be found in the literature to support this hypothesis.

In common 18–12 niobium stabilised steels, G phase seems to be found only under irradiation.[53,54] Increasing the silicon content to 6 wt-% resulted in the formation during furnace aging of niobium rich G phase, provided, however, that carbon was not available to form Cr_3Ni_2SiC. No study has been found in the literature that reports niobium rich G phase in ordinary 18–12 steels.

Ni_3Ti AND RELATED PRECIPITATES

Precipitates such as Ni_3Ti and $Ni_3(Ti,Al)$ are only found in a particular class of austenitic stainless steels: the precipitation hardening types. A typical steel in this category is A286, a 15Cr–25Ni–Al–Ti steel. These steels contain titanium and aluminium in quantities substantially larger than those in the 300 series and related compositions, to form γ' or other Ni, Ti, and/or Al precipitates, as

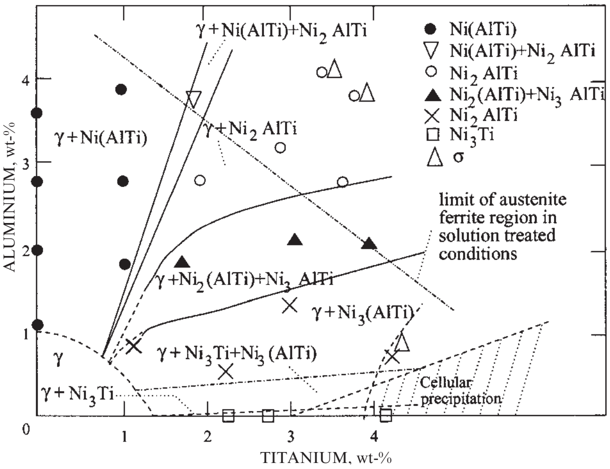

9 Effect of Al and Ti on equilibrium phases present at 800°C in 15Cr–25Ni austenitic steels[75]

summarised in Fig. 9 (Ref. 75). However, there are very few studies in which the creep properties of these steels are given attention, and long term information is not available (*see*, for example, Ref. 76). For this reason and because precipitation in these steels has been reviewed in Refs. 75 and 77, it has been decided not to cover these precipitates in depth. These are:[77]

(i) γ', which is a fcc Ni_3Al or $Ni_3(Ti,Al)$ intermetallic compound of lattice parameter 0·360 nm; it is also the transition structure of Ni_3Ti
(ii) η, which is hexagonal ($a=0{\cdot}509$ nm, $c=0{\cdot}832$ nm) and is the equilibrium structure of Ni_3Ti
(iii) β, which is NiAl, formed at lower temperatures (up to 700°C) and short aging times (10–100 h).

Other precipitates

Attention has been concentrated on precipitates most often reported and studied in creep resistant austenitic stainless steels. However, other phases are sometimes reported, depending on the alloying elements.

Cr_2N

This forms in non-stabilised austenitic stainless steels with a high nitrogen content (0·2 wt-% at 900°C with 20 wt-%Ni).[41] It has a hexagonal close packed (hcp) unit cell of lattice parameters $a=0{\cdot}478$ nm and $c=0{\cdot}444$ nm.[4] Although a major precipitate in high nitrogen non-stabilised steels, it is not found in either nitrogen bearing non-stabilised creep resistant austenitic stainless steels, because of the lower nitrogen content used, or stabilised nitrogen bearing grades, because Z phase seems to form preferentially. A detailed review of this precipitate can be found in Ref. 8.

π NITRIDE

This is reported by Jargelius-Petterson[55,59] to form in a non-stabilised 20–25 steel with 0·21 wt-%N. The composition after 10 min at 850°C is $(1{\cdot}0\pm0{\cdot}2)$Si–$(1{\cdot}1\pm0{\cdot}3)$Mn–(47 ± 1)Cr–(20 ± 1)Ni–(13 ± 1)Mo–(19 ± 1)Fe (wt-%). It has a cubic structure of lattice parameter $a=0{\cdot}63$ nm.[55]

TITANIUM CARBOSULPHIDES

The titanium carbosulphide $Ti_4C_2S_2$ is reported by Lai[49] in various type 321 steels aged at ~600°C for times between 16 000 and 53 000 h, and by Minami *et al.*[44] in a similar steel. The latter authors surmise that this phase is already present in the solution treated condition. It has an hcp structure of lattice parameter $a=0{\cdot}321$ nm and $c=1{\cdot}112$ nm.

COPPER PRECIPITATES

Little data is available concerning the effect of copper in creep resistant austenitic stainless steels. Tohyama and Minami[78] used 3 wt-% copper in Tempaloy-A1, a steel similar to 347 with the addition of a small amount of titanium. This results in precipitation of a copper rich phase, independently of the precipitation of other phases. The creep rupture strength is significantly increased in comparison with the original composition.

CHROMIUM PHOSPHIDES

The chromium phosphide Cr_3P has been reported by Rowcliffe and Nicholson[79] in an 18–10 steel with 0·3 wt-%P. It has a tetragonal unit cell with $a=0{\cdot}9186$ nm and $c=0{\cdot}4558$ nm.

Concluding remarks

An attempt has been made to review the characteristics of the main precipitates found in austenitic stainless steels, in particular wrought heat resisting grades. Precipitates forming in age hardening stainless steels have been addressed only briefly. Whereas the early stages of precipitation are fairly well understood in the usual grades of austenitic steels, this is far from the case for the new generations of nitrogen bearing stabilised austenitic steels. There is a dearth of knowledge about the phases that precipitate during long term aging, particularly with respect to thermodynamic data.

The Z phase, which plays an essential role in recent creep resistant austenitic or ferritic stainless steels, is not present in the SGTE databases commonly used with thermodynamic calculation packages such as MTDATA or Thermo-Calc. The kinetics of its formation are also rather obscure.

In discussing the stability of M_6C, there is some confusion arising from the observation that this phase is most often referred to as one particular composition of the η structure rather than the η structure itself. Similarly, thermodynamic data are only available for the molybdenum rich pole of the η structure. Other important compositions not present in the SGTE databases include Fe_3Nb_3C and Cr_3Ni_2SiX.

The formation of MX precipitates is well documented, but again, thermodynamic data are missing to model the solubility of chromium, which is likely to be important in the kinetics of precipitation. An assessment of the Cr–Nb–N system could help to improve the description of NbX precipitates, and would also provide thermodynamic data for Z phase.

Table 6 gives an overview of the structure and composition of the main precipitates in austenitic stainless steels as discussed in the present paper.

Acknowledgements

The author is grateful to D. Gooch of National Power, who funded the project of which this literature review is a part. He would also like to thank Professor A. Windle of the University of Cambridge for the provision of laboratory facilities, and his supervisor, Professor H. K. D. H. Bhadeshia, for his support, enthusiasm, and fruitful discussions.

Table 6 Crystal structures and compositions of main precipitates in austenitic stainless steels

Precipitate	Structure	Parameters, nm	Composition
NbC	fcc	$a=0{\cdot}447$	NbC
NbN	fcc	$a=0{\cdot}440$	NbN
TiC	fcc	$a=0{\cdot}433$	TiC
TiN	fcc	$a=0{\cdot}424$	TiN
Z phase	tetragonal	$a=0{\cdot}3037$, $c=0{\cdot}7391$	CrNbN
$M_{23}C_6$	fcc	$a=1{\cdot}057-1{\cdot}068$	$Cr_{16}Fe_5Mo_2C_6$ (e.g.)
M_6C	diamond cubic	$a=1{\cdot}062-1{\cdot}128$	$(FeCr)_{21}Mo_3C$, Fe_3Nb_3C, M_5SiC
σ phase	tetragonal	$a=0{\cdot}880$, $c=0{\cdot}454$	Fe–Ni–Cr–Mo
Laves phase	hexagonal	$a=0{\cdot}473$, $c=0{\cdot}772$	Fe_2Mo, Fe_2Nb
χ phase	bcc	$a=0{\cdot}8807-0{\cdot}8878$	$Fe_{36}Cr_{12}Mo_{10}$
G phase	fcc	$a=1{\cdot}12$	$Ni_{16}Nb_6Si_7$, $Ni_{16}Ti_6Si_7$

References

1. F. B. Pickering: in 'Stainless steels 84', 2–28; 1985, London, The Institute of Metals.
2. MTDATA, National Physical Laboratory, Teddington, Middlesex, UK, 1989.
3. P. Lacombe, B. Baroux, and G. Beranger (ed.): 'Stainless steels' 1993, Les Ulis, France, Éditions de Physique.
4. P. Marshall: 'Austenitic stainless steels, microstructure and mechanical properties'; 1984, London, Elsevier.
5. 'Quality and properties of NF709 austenitic stainless steel for boiler tubing applications', Technical report, Nippon Steel Corp., Tokyo, Japan, 1996.
6. J. R. Davis (ed.): 'Metals handbook', 10th edn, Vol. 1; 1990, Materials Park, OH, ASM International.
7. D. J. Naylor and W. T. Cook: 'Materials science and technology', Vol. 7; 1992, New York, VCH Publishers.
8. V. G. Gavriljuk and H. Berns: 'High nitrogen steels'; 1999, Berlin, Springer-Verlag.
9. M. Kikuchi, M. Sakabibara, Y. Otoguro, M. Mimura, T. Takahashi, and T. Fujita: Proc. Int. Conf. on 'Creep', Tokyo, Japan, April 1986, 215–220; 1986, Tokyo, Japan Society of Mechanical Engineers.
10. P. Rios: *Mater. Sci. Technol.*, 1988, **4**, 324–327.
11. P. Rios: *Mater. Sci. Eng. A*, 1991, **A142**, 87–94.
12. H. Zou and J. S. Kirkaldy: *Metall. Trans. A*, 1992, **23A**, 651–657.
13. H. Hughes: *J. Iron Steel Inst.*, 1967, **205**, 775–778.
14. H. O. Andrén, A. Henjered, and L. Karlsson: in 'Stainless steels 84', 91–96; 1985, London, The Institute of Metals.
15. H. O. Andrén, A. Henjered, and H. Norden: *J. Mater. Sci.*, 1980, **15**, 2365–2368.
16. J. Wadsworth, J. H. Woodhead, and S. R. Keown: *Met. Sci.*, 1976, **10**, 342–348.
17. S. R. Keown and F. B. Pickering: in 'Creep strength in steel and high-temperature alloys', 134–143; 1974, London, The Metals Society.
18. J. M. Adamson and J. W. Martin: *J. Iron Steel Inst.*, 1972, **210**, 271–275.
19. D. H. Jack and K. H. Jack: *J. Iron Steel Inst.*, 1972, **210**, 790–792.
20. V. Vodárek: *Metall. Mater.*, 1991, **25**, 549–552.
21. A. Raghavan, C. F. Klein, and C. N. Marzinsky: *Metall. Trans. A*, 1992, **23A**, 2455–2467.
22. P. W. Robinson and D. H. Jack: 'New developments in stainless steel technology', (ed. R. Lula), 71–76; 1985, Metals Park, OH, American Society for Metals.
23. V. Vodárek: in 'Applications of stainless steels '92', (ed. H. Nordberg and J. Björklund) Vol. 1, 123–132; 1992, Materials Park, OH, ASM International.
24. T. Thorvaldsson and G. L. Dunlop: *Met. Sci.*, 1982, **16**, 184–190.
25. G. Knowles: *Met. Sci.*, 1977, **11**, 117–122.
26. H. Uno, A. Kimura, and T. Misawa: *Corrosion*, 1992, **2**, 467–474.
27. F. R. Beckitt and B. R. Clarck: *Acta Metall.*, 1967, **15**, 113–129.
28. M. H. Lewis and B. Hattersley: *Acta Metall.*, 1965, **13**, 1159–1168.
29. T. Sourmail and H. K. D. H. Bhadeshia: Unpublished work, University of Cambridge, UK.
30. H. Tanaka, M. Murata, F. Abe, and K. Yagi: *Mater. Sci. Eng. A*, 1997, **A234**, 1049–1052.
31. L. K. Singhal and J. W. Martin: *Acta Metall.*, 1967, **15**, 1603–1610.
32. B. Sasmal: *Bull. Mater. Sci.*, 1984, **6**, 617–623.
33. B. Sasmal: *J. Mater. Sci.*, 1997, **32**, 5439–5444.
34. J. Philbert, G. Henry, M. Robert, and J. Plateau: *Mém. Sci. Rev. Métall.*, 1961, **58**, 557.
35. C. D. Cassa and V. B. Nilishwar: *J. Iron Steel Inst.*, 1969, **207**, 1003.
36. J. Ågren: *ISIJ Int.*, 1992, **32**, 291–296.
37. A. van der Ven and L. Delaey: *Prog. Mater. Sci.*, 1996, **40**, 181–264.
38. M. Hättestrand and H.-O. Andrén: *Mater. Sci. Eng. A*, 1999, **A270**, 33–37.
39. J. K. L. Lai: *Mater. Sci. Eng.*, 1983, **61**, 101–109.
40. M. Deighton: *J. Iron Steel Inst.*, 1970, **208**, 1012–1014.
41. S. Degalaix and J. Foct: *Mém. Étud. Sci. Rev. Métall.*, 1987, **84**, 645–653.
42. V. A. Biss and V. K. Sikka: *Metall. Trans. A*, 1981, **12A**, 1360–1362.
43. H. Thier, A. Baumel, and P. Schmidtmann: *Arch. Eisenhüttenwes.*, 1969, **40**, 333–339.
44. Y. Minami, H. Kimura, and Y. Ihara: *Mater. Sci. Technol.*, 1986, **2**, 795–806.
45. T. Thorvaldsson and G. L. Dunlop: *Met. Sci.*, 1980, **1**, 513–518.
46. T. Thorvaldsson and G. L. Dunlop: Proc. Int. Conf. on 'The strength of metals and alloys', Aachen, Germany, August 1979, 755–760; 1979, Oxford, Pergamon.
47. A. S. Grot and J. E. Spruiell: *Metall. Trans. A*, 1975, **6A**, 2023–2030.
48. J. Bentley and J. M. Leitnaker: in 'The metal science of stainless steels', (ed. E. W. Collings and H. W. King.), 70–91; 1978, Warrendale, PA, TMS-AIME.
49. J. K. L. Lai: *Mater. Sci. Technol.*, 1985, **1**, 97–100.
50. H. H. Stadelmaier: in 'Development in the structural chemistry of alloy phases', 141–180; 1969, New York, Plenum Press.
51. B. Weiss and R. Stickler: *Metall. Trans.*, 1972, **3**, 851–866.
52. G. Brun, J. L. Naour, and M. Vouillon: *J. Nucl. Mater.*, 1981, **101**, 109–123.
53. T. M. Williams: in 'Stainless steels 84', 403–412; 1985, London, The Institute of Metals.
54. J. M. Titchmarsh and T. M. Williams: in 'Quantitative microanalysis with high spatial resolution', (ed. G. W. Lorimer *et al.*), 223–228; 1981, London, The Institute of Metals.
55. R. F. A. Jargelius-Petterson: *Scr. Metall. Mater.*, 1993, **28**, 1399–1403.
56. J. K. L. Lai and M. Meshkat: *Met. Sci.*, 1978, **12**, 415–420.
57. J. Barcik: *Metall. Trans. A*, 1983, **14A**, 635–641.
58. L. P. Stoter: *J. Mater. Sci.*, 1981, **16**, 1039–1051.
59. R. F. A. Jargelius-Petterson: *Z. Metallkd.*, 1998, **79**, 177–183.
60. D. J. Powell, R. Pilkington, and D. A. Miller: *Acta Metall.*, 1988, **36**, 713–724.
61. Y. Minami, H. Kimura, and M. Tanimura: in 'New developments in stainless steel technology', (ed. R. Lula), 231–242; 1985, Metals Park, OH, American Society for Metals.
62. R. Sumerling and J. Nutting: *J. Iron Steel Inst.*, 1965, **203**, 398–405.
63. V. Ramaswamy and D. R. F. West: *J. Iron Steel Inst.*, 1970, **208**, 391–394.
64. T. M. Williams and J. M. Titchmarsh: *J. Nucl. Mater.*, 1981, **98**, 223–226.

65. D. J. POWELL, R. PILKINGTON, and D. A. MILLER: in 'Stainless steels 84', 382–390; 1985, London, The Institute of Metals.
66. R. C. ECOB, R. C. LOBB, and V. L. KOHLER: *J. Mater. Sci.*, 1987, **22**, 2867–2880.
67. J. BARCIK: *Mater. Sci. Technol.*, 1988, **4**, 5–15.
68. L. R. WOODYATT, C. T. SIMS, and H. J. BEATTIE: *Trans. AIME*, 1966, **236**, 519.
69. A. W. DENHAM and J. M. SILCOCK: *J. Iron Steel Inst.*, 1969, **207**, 585–592.
70. J. K. L. LAI: *Mater. Sci. Eng.*, 1983, **58**, 195–209.
71. W. E. WHITE and I. LE MAY: *Metallography*, 1970, **3**, 51–60.
72. H. J. BEATTIE and W. C. HAGEL: *J. Met.*, 1957, 911–917.
73. H. J. BEATTIE and F. L. VERSNYDER: *Nature*, 1956, **178**, 208.
74. R. A. P. DEWEY, G. SUMMER, and I. S. BRAMMAR: *J. Iron Steel Inst.*, 1965, **203**, 938–944.
75. F. B. PICKERING: in 'The metallurgical evolution of stainless steels', (ed. F. B. Pickering), 391–401; London, 1979, The Metals Society.
76. D. V. V. SATYANARAYANA, M. C. PANDEY, and D. M. R. TAPLIN: *Trans. Indian Inst. Met.*, 1996, **49**, 419–423.
77. E. J. DULIS: in 'The metallurgical evolution of stainless steels', (ed. F. B. Pickering), 420–441; 1979, London, The Metals Society.
78. A. TOHYAMA and Y. MINAMI: in 'Advanced heat resistant steels for power generation', (ed. R. Viswanathan and J. Nutting), 494–506; 1999, London, IoM Communications Ltd.
79. A. F. ROWCLIFFE and R. B. NICHOLSON: *Acta Metall.*, 1972, **20**, 143–155.